Metal−Organic Chemical Vapor Deposition of Indium Selenide Thin Films

Sarah L. Stoll† and Andrew R. Barron*

Department of Chemistry and Department of Mechanical Engineering and Materials Science, Rice University, Houston, Texas 77005

Received September 24, 1997. Revised Manuscript Received November 25, 1997

Indium selenide (InSe) thin films have been grown at 230−420 °C by low-pressure metal−organic chemical vapor deposition (MOCVD) using the single-source precursors $[(^tBu)_2In(\mu\text{-}Se^tBu)]_2$ and $[(Me_2EtC)In(\mu_3\text{-}Se)]_4$. Characterization of the films by energy-dispersive X-ray analysis (EDX) showed those grown from $[(^tBu)_2In(\mu\text{-}Se^tBu)]_2$ to be indium rich, while those grown from $[(Me_2EtC)In(\mu_3\text{-}Se)]_4$ are stoichiometric InSe. Transmission electron microscopy (TEM) indicates that the film morphology and crystallinity are highly dependent on the precursor and the deposition temperature. At low temperatures <330 °C ball-like morphologies are observed, while deposition at 350−370 °C results in highly crystalline textured films. Use of $[(^tBu)In(\mu_3\text{-}Se)]_4$ as the precursor at 320−420 °C results in indium metal films. The relationship between the precursor's structure and the film's morphology and chemical composition are discussed. The efficacy of the single-source precursor approach is considered with respect to elemental composition, phase formation, and film morphology.

Introduction

Recent work from our laboratory has been concerned with the thin-film growth by metal organic chemical vapor deposition (MOCVD) of the group 13 chalcogenides.[1] In this regard we have been interested in the control exerted by a precursor's molecular structure over the composition,[2] structure,[3] and morphology[4] of a thin film. Previous studies have focused on gallium and indium sulfide precursors in which the molecular M_nS_n core (M = Ga, In) is retained during MOCVD conditions.[3a,b] We have proposed that this effect is due to the strength of the M−S bonds and consequently the stability of the molecular core. In contrast, the weaker M−Se and M−Te bonds should reduce the stability of the M_nE_n core during MOCVD and thus reduce the molecular control exerted by the precursor.[5] In this regard our results for the MOCVD growth of gallium selenide and gallium telluride thin films are reported elsewhere,[6] while those for the indium are the subject of this paper.

The indium selenides, InSe and In_2Se_3, consist of hexagonal layered structures, and both compositions exhibit a number of polytypes;[7] the structural differences arising from the stacking order of the layers, manifested in a variation of the length of the crystallographic *c*-axis.[8] Both InSe and In_2Se_3 have band gaps in the range 1.1−1.5 eV,[9] which make them suitable materials for optoelectronic[10] and photovoltaic applications.[11] Electronic applications such as nonlinear mixing frequency devices has also been considered.[12] As a result of the layered structure, InSe has been proposed as a suitable electrode material for Li microbatteries.[13] Another consequence of the layered structure is a strong anisotropy in the conductivity in InSe.[14] Finally, the absence of dangling bonds on the (001) surface of InSe allows for its potential use for heterojunction device applications with a low density of interface states.[15]

* To whom correspondence should be addressed.
† Present address: Department of Chemistry, Oberlin College, Oberlin, OH 44074.

(1) Barron, A. R. *Adv. Mater. Opt. Electron.* **1995**, *5*, 245.
(2) (a) MacInnes, A. N.; Power, M. B.; Hepp, A. F.; Barron. A. R. *J. Organomet. Chem.* **1993**, *449*, 95. (b) Shulz, S.; Gillan, E. G.; Rogers, L. M.; Rogers, R.; Barron, A. R. *Organometallics* **1996**, *15*, 4880.
(3) (a) MacInnes, A. N.; Power, M. B.; Barron, A. R. *Chem Mater.* **1992**, *4*, 11. (b) MacInnes, A. N.; Power, M. B.; Barron, A. R. *Chem. Mater.* **1993**, *5*, 1344. (c) MacInnes, A. N.; Cleaver, W. M.; Barron, A. R.; Power, M. B.; Hepp, A. F. *Adv. Mater. Opt. Electron.* **1992**, *1*, 229.
(4) Stoll, S. L.; Gillan, E. G.; Barron, A. R. *Chem. Vapor Deposition* **1996**, *2*, 182.
(5) Thermochemical bond energies: Ga−S (318 kJ mol^{-1}), Ga−Se (274 kJ.mol^{-1}), and Ga−Te (251 kJ mol^{-1}).
(6) Gillan E. G.; Barron, A. R. *Chem. Mater.* **1997**, *9*, 3037.
(7) The electronic properties of each indium selenide are also dependent on the polytype, see for example: (a) Likforman, A.; Fourcroy, P. H.; Guittard, M.; Flahant, J.; Poirier, R.; Szydlo, N. *J. Solid State Chem.* **1980**, *33*, 91. (b) Julien, C.; Chevy, A.; Siapkas, D. *Phys. Status Solidi A* **1990**, *118*, 553. (c) Persin, M.., Persin, A.; Celustka, B. *Thin Solid Films* **1972**, *11*, 153.
(8) Lattice parameters for InSe: a = 4.00 and c = 25−74 Å; In_2Se_3: a = 4.025, c = 9.6−28.5 Å.
(9) McCanny, J. V.; Murray, R. B., *J. Phys. C* **1979**, *10*, 1211.
(10) Ando, K.; Katsui, A. *Thin Sold Films* **1981**, *76*, 141.
(11) (a) Segura, A.; Chevy, A.; Guesdon, J. P.; Besson, J. M. *Solar Energy Mater.*, **1980**, *2*, 159. (b) Nang, T. T.; Matsushita, T.; Okuda, M.; Suzuki, A. *Jpn. J. Appl. Phys.* **1977**, *16*, 153. (c) Guesdon, J. P.; Kobbi, B.; Julien, C.; Balkanski, M. *Phys. Status Solidi A* **1987**, *102*, 327. (d) Ando, K.; Katsui, A. *Thin Solid Films* **1981**, *76*, 141.
(12) Oudar, J. L.; Kupecek, P. J.; Chemla, D. S. *Opt. Commun.* **1979**, *29*, 119.
(13) (a) Julien, C.; Massot, M.; Dzwonkowski, P.; Emery, J. Y.; Balkanski, M. *Infrared Phys.* **1989**, *29*, 769. (b) Balkanski, M.; Julien, C.; Emery, J. Y. *J. Power Sources* **1989**, *26*, 615. (c) Samaras, I.; Julien, C.; Balkanski, M. *Solid State Microbatteries, NATO ASI Series, Ser. B* **1990**, *217*, 293. (d) Whittingan, M. S. *Prog. Solid State Chem.* **1978**, *12*, 41.
(14) (a) Camassel, J.; Merle, P.; Mathieu, H.; Chevy, A. *Phys. Rev. B* **1978**, *17*, 4718. (b) Julien, C.; Eddrief, M.; Kambas, K.; Balkanski, M. *Thin Solid Films* **1986**, *27*, 137. (c) Sastry D. V. K.; Reddy, P. J. *Thin Solid Films* **1983**, *105*, 139.

S0897-4756(97)00638-8 CCC: $15.00
Published on Web 01/30/1998

There have been a number of methods reported for the growth of indium selenide thin films, of which vacuum evaporation has been studied in the greatest detail.[16] Other methods include: flash evaporation,[17] MBE,[18] reaction of selenium with InP,[19] or In_2O_3,[20] surfaces, electrochemical synthesis,[21] solid-state pyrolysis of chemical precursors,[22] and metal organic chemical vapor deposition (MOCVD).,[23−25] Potentially, MOCVD is the most advantageous method for film growth of the indium selenides for semiconductor device applications. However, while In_2Se_3 has been successfully grown by MOCVD using $In(SeR)_3$ [R = Ph,[23] $C(SiMe_3)_3$[24]] and $In[Se_2CNMe(n\text{-hexyl})]_3$[25] as single-source precursors, the growth of *phase-pure* InSe has not been observed despite the use of a single-source precursor containing an In:Se ratio of 1:1, i.e., $[Me_2In(\mu\text{-SePh})]_2$.[26]

We have previously reported[4] that thin films of stoichiometric indium sulfide (InS) may be grown using the related dimeric monothiolate complexes $[(R)_2In(\mu\text{-}S^tBu)]_2$ (R = ^{n}Bu, ^{t}Bu). On the basis of these results, we proposed to investigate the growth by MOCVD of InSe thin films using the selenolate compound $[(^tBu)_2In(\mu\text{-}Se^tBu)]_2$ (**I**). One disadvantage of selenolate compounds as MOCVD precursors is the presence of a relatively strong Se−C bond (ca. 240 kJ mol^{-1}), which are potentially a source for carbon contamination in the deposited films. A better solution is to employ precursors without Se−C bonds. Thus, we have also investigated the use of the indium selenide cubane precursors, $[(R)In(\mu_3\text{-Se})]_4$, R = ^{t}Bu, CMe_2Et (**II**). In a preliminary communication, we reported the MOCVD of nanoparticles of InSe using the cubane precursor $[(Me_2EtC)In(\mu_3\text{-Se})]_4$.[4] We now describe full details of the MOCVD of InSe thin films.

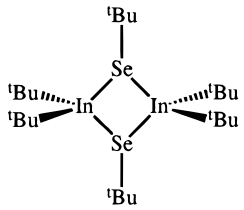

(**I**)

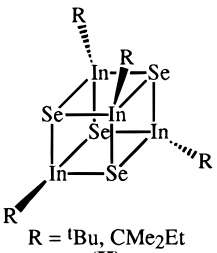

(**II**)

Table 1. Summary of Deposition Conditions for Indium Selenide Single-Source Precursors

precursor	$[(^tBu)_2In(\mu\text{-}Se^tBu)]_2$	$[(^tBu)In(\mu_3\text{-Se})]_4$	$[(Me_2EtC)In(\mu_3\text{-Se})]_4$
precursor temp. (°C)	170	80	160
chamber base pressure (Torr)	10^{-3}	10^{-3}	10^{-3}
carrier gas	argon	argon	argon
flow rate (mL min^{-1})	n/a	500−900	100−950
substrate	Si(100), KBr	Si(100), quartz	Si(100), KBr
substrate temp (°C)	330−370	320−420	230−350

Results and Discussion

The precursors, $[(^tBu)_2In(\mu\text{-}Se^tBu)]_2$, $[(^tBu)In(\mu_3\text{-Se})]_4$, and $[(Me_2EtC)In(\mu_3\text{-Se})]_4$, were prepared by previously reported methods.[27] Thermogravimetric and differential thermal analyses (TG/DTA) were performed under a dynamic vacuum (10 mTorr)[28] as well as an inert (dry argon) atmosphere, to determine the volatilization−decomposition window for each precursor.

Thin-film growth was carried out on single-crystal KBr, p-type Si (100), and fused quartz glass substrates in a hot-walled horizontal glass MOCVD system as previously described.[29] The deposition experiments were carried out either under low pressure in a purified argon flow at a chamber base pressure of (1 mTorr) or under dynamic vacuum. A summary of the deposition parameters is given in Table 1. The films were all contiguous by SEM and showed uniform coverage. No appreciable difference in the gross morphology of the film as a function of substrate was noted. However, the microstructure was found to be highly dependent on the identity of the precursor and the deposition temperature. This relationship is summarized in Table 2 and detailed below for each of the precursor systems.

$[(^tBu)_2In(\mu\text{-}Se^tBu)]_2$. As can be seen from Figure 1a, $[(^tBu)_2In(\mu\text{-}Se^tBu)]_2$ readily sublimes (T_{sub} = 151 °C) under vacuum with ca. 96% of the material volatilized. In contrast, no volatility is observed at atmospheric pressure (Figure 1b), with decomposition occurring at high temperatures (216 °C). The overall mass loss (48%) is consistent with the loss of the *tert*-butyl groups and the formation of InSe (calcd mass loss = 47%). The X-ray diffraction (XRD) analysis (Figure 2) of the residue from the TGA experiment is consistent with hexagonal InSe (JCDPS No. 12-118). While we have insufficient data to determine the mechanism of decomposition, we note that the two decomposition steps observed in the TGA of $[(^tBu)_2In(\mu\text{-}Se^tBu)]_2$ are numeri-

(15) See for example: (a) Matsushita, T.; Nang, T. T.; Okuda, M.; Suzuki, A.; Yokota, S. *Jpn. J. Appl. Phys.* **1976**, *15*, 901. (b) Tatsuyama, C.; Tanbo, T.; Nakayama, N. *Appl. Surf. Sci.* **1989**, *41/42*, 539. (c) Martinez-Pastor, J.; Segura, A.; Valdes, J. L.; Chevy, A. *J. Appl. Phys.* **1987**, *62*, 1477.

(16) (a) Persin, M.; Celustka, B.; Markovic, B.; Persin, A. *Thin Solid Films* **1970**, *5*, 123. (b) Sharma, S. K. *Thin Solid Films* **1971**, *11*, 201. (c) Persin, M.; Persin, A.; Celustka, B. *Thin Solid Films* **1972**, *12*, 117. (d) Fitzgerald, A. G. *Thin Solid Films* **1972**, *13*, S5. (e) Chaudhuri, S.; Biswas, S. K.; Choudhury, A. *Solid State Commun.* **1985**, *53*, 273. (f) Igasaki, Y.; Yamauchi, H.; Okamura, S. *J. Cryst. Growth.* **1991**, *112*, 797. (g) Parlak, M.; Erçelebi, Ç.; Günal, I.; Salaeva, Z.; Allakhverdiev, K. *Thin Solid Films* **1995**, *258*, 86. (h) Yudasaka, M.; Nakanishi, K.*Thin Solid Films* **1987**, *155*, 145.

(17) Guesdon, J. P.; Kobbi, B.; Julien, C.; Balkanski, M. *Phys. Status Solidi A* **1987**, *102*, 327.

(18) (a) Emery, J. Y.; Brahim-Otsmane, L.; Jouanne, M.; Julien, C.; Balkanski, M. *Mater. Sci. Eng.* **1989**, *B3*, 13. (b) Emery, J. Y.; Julien, C.; Jouanne, M.; Balkanski, M. *Appl. Surf. Sci.* **1988**, *33/34*, 619. (c) Yudasaka, M.; Matsuoka, T.; Nakanishi, K. *Thin Solid Films* **1987**, *146*, 65.

(19) Srivastava G. P.; Umerski, A. *Surf. Sci.* **1995**, *331*, 590.

(20) Weng, S.; Wynands, H.; Cocivera, M. *Chem. Mater.* **1992**, *4*, 1428.

(21) Herrero J.; Ortega, J. *Solar Energy Mater.* **1987**, *16*, 477.

(22) (a) Hepp, A. F.; Hehemann, D. G.; Duraj, S. A.; Clark, E. B.; Eckles, W. E.; Fanwick, P. E. *Mater. Res. Soc., Symp. Proc.* **1994**, *327*, 29. (b) Dhingra S.; Kanatzidis, M. G. *Mater. Res. Soc., Symp. Proc.* **1990**, *180*, 825. (c) Kanatzidis, M. G.; Dhingra S. *Inorg. Chem.* **1989**, *28*, 2024.

(23) Gysling, H. J.; Wernberg, A. A.; Blanton, T. N. *Chem. Mater.* **1992**, *4*, 900.

(24) Cheon, J.; Arnold, J.; Yu, K.-M.; Bourret, E. D. *Chem. Mater.* **1995**, *7*, 2273.

(25) O'Brien, P.; Otway, D. J.; Walsh, J. R. *Chem. Vap. Deposition* **1997**, *3*, 227.

(26) While the In/Se ratio of films grown from $[Me_2In(\mu\text{-SePh})]_2$ at high temperature (408−477 °C) was close to stoichiometric InSe (In/Se = 1.05) a second crystalline phase, In_xSe_y, was observed; see ref 23.

(27) Stoll, S. L.; Bott, S. G.; Barron, A. R. *J. Chem. Soc., Dalton Trans.* **1997**, 1315.

(28) Non-SI units: 1 Torr = 1 mmHg = 133 Pa.

(29) Landry, C. C.; Cheatham, L. K.; MacInnes, A. N.; Barron, A. R. *Adv. Mater. Opt. Electron.* **1992**, *1*, 3.

Table 2. Dependence of the Composition and Morphology of MOCVD Grown Indium Selenide Thin Films on the Precursor and Deposition Temperature

precursor	deposition temp (°C)	analysis (In:Se)	crystalline phase	morphology
$[(^t\text{Bu})_2\text{In}(\mu\text{-Se}^t\text{Bu})]_2$	330	57:43	h-InSe	balls and needles
	350	55:45	h-InSe	needles
	370	58:42	h-InSe	textured
$[(^t\text{Bu})\text{In}(\mu_3\text{-Se})]_4$	320	100:0	In metal	smooth
	420	100:0	In metal	smooth
$[(\text{Me}_2\text{EtC})\text{In}(\mu_3\text{-Se})]_4$	230	52:48	h-InSe[a]	balls
	260	50:50	h-InSe[a]	balls
	290	50:50	h-InSe	balls
	350	50:50	h-InSe	textured

[a] Poorly crystalline.

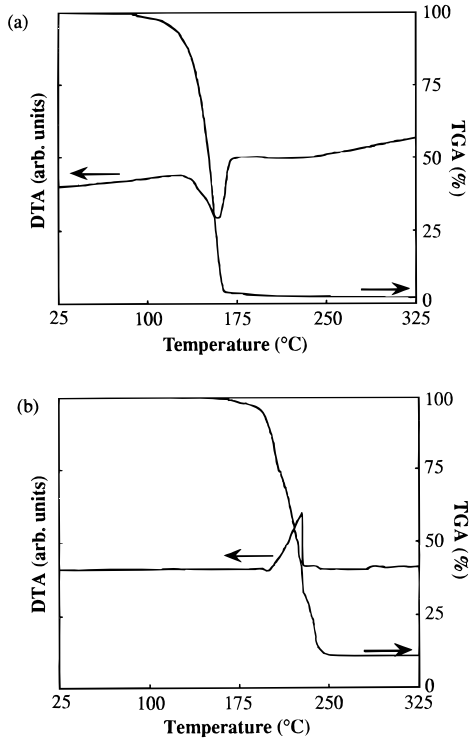

Figure 1. Thermogravimetric analysis (TGA, right-hand axis) and differential thermal analysis (DTA, left-hand axis) of $[(^t\text{Bu})_2\text{In}(\mu\text{-Se}^t\text{Bu})]_2$ under (a) dynamic vacuum and (b) flowing nitrogen, see text for discussion.

cally consistent with the stepwise loss of two *tert*-butyl groups at 216 °C followed by a third *tert*-butyl group at 238 °C.

While $[(^t\text{Bu})_2\text{In}(\mu\text{-Se}^t\text{Bu})]_2$ exhibits volatility under vacuum over the temperature range 106−170 °C, the lack of significant decomposition allows for mass transport to be maximized by use of the upper end of the temperature range. Thin-film growth using $[(^t\text{Bu})_2\text{In}(\mu\text{-Se}^t\text{Bu})]_2$ was therefore carried out at low pressure with a precursor heated to 170 °C; see Table 1.

On the basis of energy-dispersive X-ray (EDX) analysis, the films are selenium deficient, with an In/Se ratio in the range 1.22−1.42. It is interesting to note that while the observed In/Se ratio is close to that of In_4Se_3 (i.e., In/Se = 1.33); however, no evidence of the latter phase has been found by X-ray diffraction. The formation of indium-rich (selenium-deficient) films may be a result of two possible effects. Yudasaka et al.[30] have previously reported that when indium and selenium are

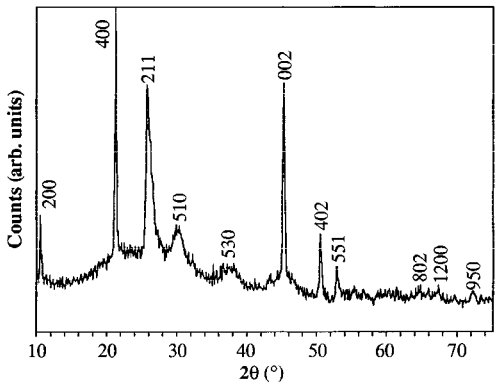

Figure 2. XRD of InSe powder prepared from the solid state thermolysis of $[(^t\text{Bu})_2\text{In}(\mu\text{-Se}^t\text{Bu})]_2$ at 550 °C. Hexagonal InSe peaks are indexed.

evaporated individually in a 1:1 ratio onto a substrate at elevated temperatures (>240 °C) selenium is not deposited at all due to its relatively high volatility. Thus, with an InSe ratio of 1:1 dictated by the precursor, $[(^t\text{Bu})_2\text{In}(\mu\text{-Se}^t\text{Bu})]_2$, it is possible that the same volatility effects occur during MOCVD as are observed for thermal evaporated film growth. However, given that films grown from $[(\text{Me}_2\text{EtC})\text{In}(\mu_3\text{-Se})]_4$ (see below) under similar conditions are stoichiometric additional factors must be considered. In this regard, we have previously reported that deposition at 300−350 °C of indium sulfide films using $[(^t\text{Bu})_2\text{In}(\mu\text{-S}^t\text{Bu})]_2$ as a single-source precursor (i.e., In:S in the precursor = 1:1) have a composition equivalent to In_2S. On the basis of analysis of the volatile side products, we proposed that this elemental imbalance was due to the surface formation and subsequent volatilization of $^t\text{BuSS}^t\text{Bu}$. Likewise, if a similar reaction occurred for the selenium analogue, $[(^t\text{Bu})_2\text{In}(\mu\text{-Se}^t\text{Bu})]_2$, i.e., formation of $^t\text{BuSeSe}^t\text{Bu}$, then indium-rich films would result.[31]

The as-deposited films were floated off KBr wafers and analyzed by transmission electron microscopy (TEM). Figure 3a shows the bright field image of the film obtained from $[(^t\text{Bu})_2\text{In}(\mu\text{-Se}^t\text{Bu})]_2$ grown at 330 °C. The films consist of a mixture of near spherical particles and needles. The spherical particles have a mean diameter of 88 nm, while the needles grow up to 450 nm in length. The selected area electron diffraction pattern of the needles exhibits well-defined grid, superimposed upon a series of weak rings, both of which may be indexed to hexagonal InSe (JCDPS No. 12-118) and is similar to previous electron diffraction studies of InSe.[32] Needles are the dominant morphology in films deposited at 350 °C, as indicated by the bright-field TEM image shown in Figure 3b. A defined set of growth directions (i.e., coplanar with the substrate) may be visually identified. This is reflected in the selected-area electron diffraction pattern (Figure 4), where despite the polycrystalline nature of the film, a well-defined spot pattern indicative of preferred orientation is obtained. Crystal growth

(30) Yudasaka, M.; Matsuoka, T.; Nakanishi, K. *Thin Solid Films* **1987**, *146*, 65.

(31) An alternative, but less likely, explanation for the observation of indium-rich films may be that the precursor, $[(^t\text{Bu})_2\text{In}(\mu\text{-Se}^t\text{Bu})]_2$, undergoes a ligand redistribution reaction to form $\text{In}(^t\text{Bu})_3$, whose decomposition would result in the formation of an In-rich film.

(32) Schubert, K.; Dörre, E.; Günzel, E. *Naturwissenschaften* **1954**, *41*, 488.

Figure 3. Bright-field TEM image of an InSe film grown at (a) 330 °C, (b) 350 °C, and (c) 370 °C, using $[(^t\text{Bu})_2\text{In}(\mu\text{-Se}^t\text{Bu})]_2$.

does not continue at higher temperatures; a further increase in the deposition temperature (370 °C) results in the growth of a textured film (Figure 3c), whose

Figure 4. Selected area electron diffraction pattern of an InSe film grown at 350 °C using $[(^t\text{Bu})_2\text{In}(\mu\text{-Se}^t\text{Bu})]_2$.

electron diffraction is dominated by narrow rings indicative of a polycrystalline film with no preferred orientation.

The formation of near spherical particles of InSe deposited at 330 °C suggests a vapor-phase decomposition accompanies deposition during the film growth at this temperature; vide infra for $[(\text{Me}_2\text{EtC})\text{In}(\mu_3\text{-Se})]_4$. In contrast, the formation of oriented needlelike crystals for films grown at 350 °C requires that surface decomposition of $[(^t\text{Bu})_2\text{In}(\mu\text{-Se}^t\text{Bu})]_2$ dominate the growth kinetics. Furthermore, the formation of textured polycrystalline films with small grains at the highest deposition temperature studied (370 °C) suggests that the surface growth rate is sufficiently rapid to preclude extended crystal growth.

$[(^t\text{Bu})\text{In}(\mu_3\text{-Se})]_4$. Although the cubane compound, $[(^t\text{Bu})\text{In}(\mu_3\text{-Se})]_4$, sublimes under vacuum (T_{sub} = 151 °C), it does so with volatilization of only 82% of the starting material, suggestive of decomposition accompanying sublimation (see Figure 5a). Under flowing nitrogen the TGA of $[(^t\text{Bu})\text{In}(\mu_3\text{-Se})]_4$ shows a mass loss consistent with decomposition and sublimation over the range 156−211 °C (see Figure 5b). As a consequence of the decomposition observed for $[(^t\text{Bu})\text{In}(\mu_3\text{-Se})]_4$, even under vacuum, the precursor temperature was limited to 80 °C the lowest end of the sublimation range 74−147 °C.

Thin-film growth using $[(^t\text{Bu})\text{In}(\mu_3\text{-Se})]_4$ was carried out on p-type (100) oriented silicon and quartz substrates using the chamber configuration used for $[(^t\text{Bu})_2\text{In}(\mu\text{-Se}^t\text{Bu})]_2$. A summary of the deposition conditions is given in Table 1. The as-deposited films were black and metallic looking and by microprobe analysis were devoid of selenium. The XRD showed the films to be polycrystalline indium metal (JCDPS No. 5-642).

The deposition of indium metal as opposed to indium selenide for film growth using $[(^t\text{Bu})\text{In}(\mu_3\text{-Se})]_4$ is perhaps surprising given the successful growth of InSe

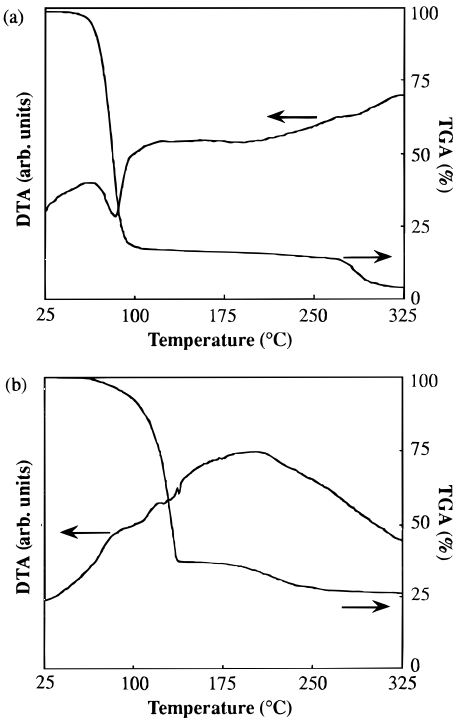

Figure 5. Thermogravimetric analysis (TGA, right-hand axis) and differential thermal analysis (DTA, left-hand axis) of [(^{t}Bu)In(μ_3-Se)]$_4$ under dynamic vacuum (a) and flowing nitrogen (b), see text for discussion.

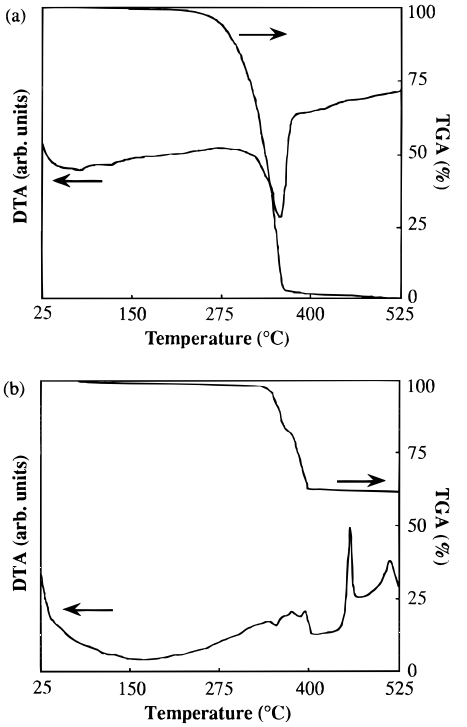

Figure 6. Thermogravimetric analysis (TGA, right-hand axis) and differential thermal analysis (DTA, left-hand axis) of [(Me_2EtC)In(μ_3-Se)]$_4$ under (a) dynamic vacuum and (b) flowing nitrogen, see text for discussion.

using the *tert*-amyl analogue, [(Me_2EtC)In(μ_3-Se)]$_4$, under similar conditions; see below. However, it is possible that the *tert*-butylcubane is more susceptible to core cleavage at the high temperatures required for film growth.[33] Catastrophic core cleavage (i.e., cleavage of all In−Se bonds) may explain the deposition of indium metal in a manner similar to that discussed in the previous section for the loss of selenium during thermal evaporation of elemental indium and selenium. When evaporation of In and Se metals as separate sources is carried out at high temperatures, no selenium is incorporated into the deposited film.[30] However, an alternative explanation may involve the thermal decomposition of [(^{t}Bu)In(μ_3-Se)]$_4$ to give elemental selenium and a monovalent indium compound (eq 1). Decomposition of

$$[(^t\text{Bu})\text{In}(\mu_3\text{-Se})]_4(g) \rightarrow \text{“}(^t\text{Bu})\text{In”(surface)} + \text{Se}(g) \quad (1)$$

$$[\{(\text{Me}_3\text{Si})_2\text{HC}\}\text{In}]_4 + 4\text{E} \xrightarrow[\text{E = S, Se, Te}]{} [\{(\text{Me}_3\text{Si})_2\text{HC}\}\text{In}(\mu_3\text{-E})]_4 \quad (2)$$

the fragment “(^{t}Bu)In” would lead to In films. While we have no direct evidence for such a reaction, we note that the reverse reaction is employed in the synthesis of the indium chalcogenide cubanes, [{($Me_3Si)_2$HC}In(μ_3-Se)]$_4$, eq 2.[34] The observation of an orange region (elemental Se) down stream of the deposition zone, is consistent with this explanation.

[(Me_2EtC)In(μ_3-Se)]$_4$. The cubane compound, [(Me_2EtC)In(μ_3-Se)]$_4$, sublimes under vacuum (T_{sub} = 220 °C), without significant decomposition (Figure 6a). However, thermolysis under atmospheric pressure results in both sublimation and decomposition at 218 °C (Figure 6b). The overall mass loss (38%) under atmospheric pressure is consistent with slight sublimation and loss of the *tert*-amyl groups and the formation of InSe (calcd mass loss = 27%). The XRD analysis of the residue (Table 3) from the TGA experiment is consistent with hexagonal-InSe (JCDPS No. 12-118). It is interesting that the large exotherm (at 288 °C) observed in the DTA (Figure 6b) is consistent with the crystallization of

Table 3. Comparison of Hexagonal-InSe Formed from [(Me_2EtC)In(μ_3-Se)]$_4$ by Solid-State Thermolysis and MOCVD.

hexagonal InSe (JCDPS 12-118)			solid-state thermolysis T_{dec} = 350 °C	MOCVD T_{dep} = 350 °C
hkl	I/I_0	*d*, Å	*d*, Å[a]	*d*, Å[b]
002	40	8.36	8.31[c]	
400	100	4.16	4.16	3.92
211	80	3.38	3.46	3.56
420	20	3.14		3.13
221	40	3.05	*d*	
510	40	2.96	2.96	2.90
600	20	2.77		2.60
421	40	2.44	*d*	
530	40	2.38	*d*	
620	20	2.30		
800	20	2.08		2.09
002	100	2.00	2.00	2.04
810	20	1.95		1.94
402	40	1.80	1.80	1.81
551	20	1.73	1.73	1.74
602	20	1.62		1.65
802	20	1.44	1.44	1.46
1021	20	1.40		
1200	40	1.39	1.37	
950	20	1.35	1.31	1.34

[a] X-ray diffraction (Cu Kα). [b] Electron diffraction. [c] Broad rings. [d] High *d* spacing are obscured by amorphous halo.

(33) No film growth was observed below 300 °C for [(^{t}Bu)In(μ_3-Se)]$_4$.
(34) (a) Uhl, W.; Graupner, R.; Layh, M.; Schütz, U. *J. Organomet. Chem.* **1995**, *93*, C1. (b) Uhl, W.; Graupner, R.; Pohlmann, M.; Pohl, S.; Saak, W. *Chem. Ber.* **1996**, *129*, 143.

hexagonal-InSe from indium selenium mixtures in which the In:Se ratio is 1.[35]

Thin-film growth using $[(Me_2EtC)In(\mu_3\text{-}Se)]_4$ was carried out under a dynamic vacuum with a precursor heated to 160 °C; see Table 1. The composition of the deposited films (In:Se) was determined by energy-dispersive EDX analysis to be 50:50 (±2%). Thin films grown on KBr substrates were analyzed by TEM. The films grown at 230−290 °C consist of spheres; see Figure 7a. The size of the spherical particles within experimental error appears to be independent of the growth temperature, having a mean diameter of 88 nm and a standard deviation of 30 nm. The selected area electron diffraction pattern exhibits broad rings consistent with a poorly crystalline material, e.g., Figure 7b. However, the rings become increasingly well-defined with increased deposition temperature.

The small sizes and pseudospherical geometry of the InSe particles suggests a vapor-phase component is operative during the deposition of these metal selenide films. It is likely that the fragmentation of the cubane precursors in the vapor phase yields highly reactive molecular species. These fragments may combine to form particles that will remain in the vapor phase until their size is such as to "precipitate" out of the gas stream. The deposition of particles from the vapor phase due to gravitational or thermophoretic forces has been studied for SiC.[36] By comparison based on the relative density, we expect gravitational forces to dominate for InSe particles greater than 80 μm in diameter. At the low deposition temperatures employed in the present study, continued particle growth on the surface should be limited. Factors that may control the particle size include precursor concentration, vacuum versus atmospheric growth, growth temperature, and the thermal stability of the precursor.

In contrast to the films grown at 230−290 °C, deposition at 350 °C produces highly crystalline textured films (Figure 8a), whose selected area electron diffraction pattern (Figure 8b) exhibits a well-defined grid, superimposed upon a series of weak rings, both of which may be indexed to hexagonal InSe (JCDPS No. 12-118, Table 3). The formation of the hexagonal phase of InSe suggests that a core cleavage is occurring during the decomposition of $[(Me_2EtC)InSe]_4$. Unlike the Ga_4S_4 core in $[(^tBu)GaS]_4$, the weaker In−Se bonds in $[(Me_2EtC)InSe]_4$ are consistent with cleavage in the vapor phase. The cleavage of the precursor's In_4Se_4 core is presumably occurring in the vapor phase at the elevated deposition temperatures used here. We have previously proposed that the growth of highly oriented hexagonal-GaSe and GaTe from $[(R)Ga(\mu_3\text{-}E)]_4$ (E = Se and Te, respectively) is due to the formation of "$(R)_3Ga_3E_3$" fragment.[6] Clearly, a similar decomposition may occur for $[(Me_2EtC)In(\mu_3\text{-}Se)]_4$.

What Is the Value of Single-Source Precursors? The rationalization most commonly offered for the single-source precursors approach has been that the presence of covalent bonds between the required elements in the desired atomic ratio offers an efficient manner to transport multiple elements, with different volatilities, to the film growth surface. It has been suggested that the important factors to be considered in the design of single-source precursors are, in addition to containing the desired elements, they should preferentially contain ligands that are readily removed during film growth and should be sufficiently volatile to allow vapor transport at appropriate temperatures. As noted in the Introduction, our interest in single-source precursors has been driven by the desire to understand the

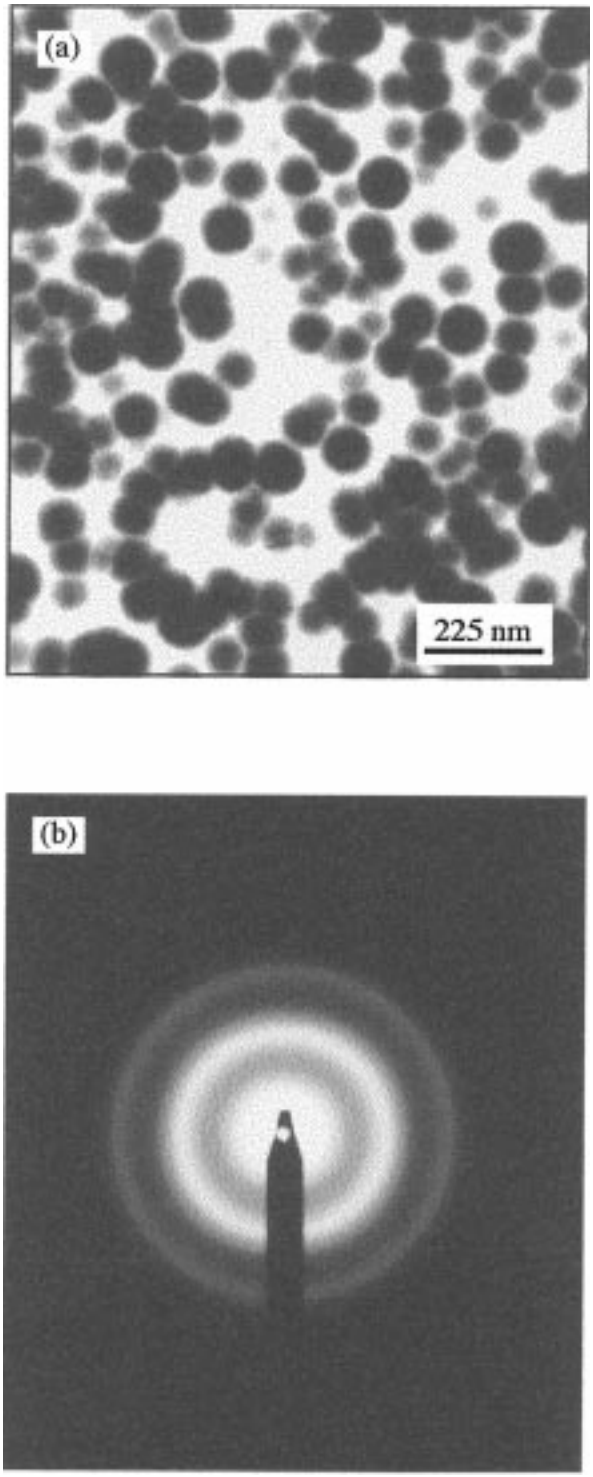

Figure 7. Bright-field TEM image (a) and associated selected area electron diffraction pattern (b) of an InSe film grown at 290 °C using $[(Me_2EtC)In(\mu_3\text{-}Se)]_4$.

(35) It is has been found that the temperature at which InSe crystallizes is highly dependent on the ratio of In:Se, see: Oyelaran, O.; Novet, T.; Johnson, C. D.; Johnson, D. C. *J. Am. Chem. Soc.* **1996**, *118*, 2422.

(36) Allendoy, M. D.; Hurt, R. H.; Young, N.; Reagon, P.; Robbins, M. *J. Mater. Res.* **1993**, *8*, 1651.

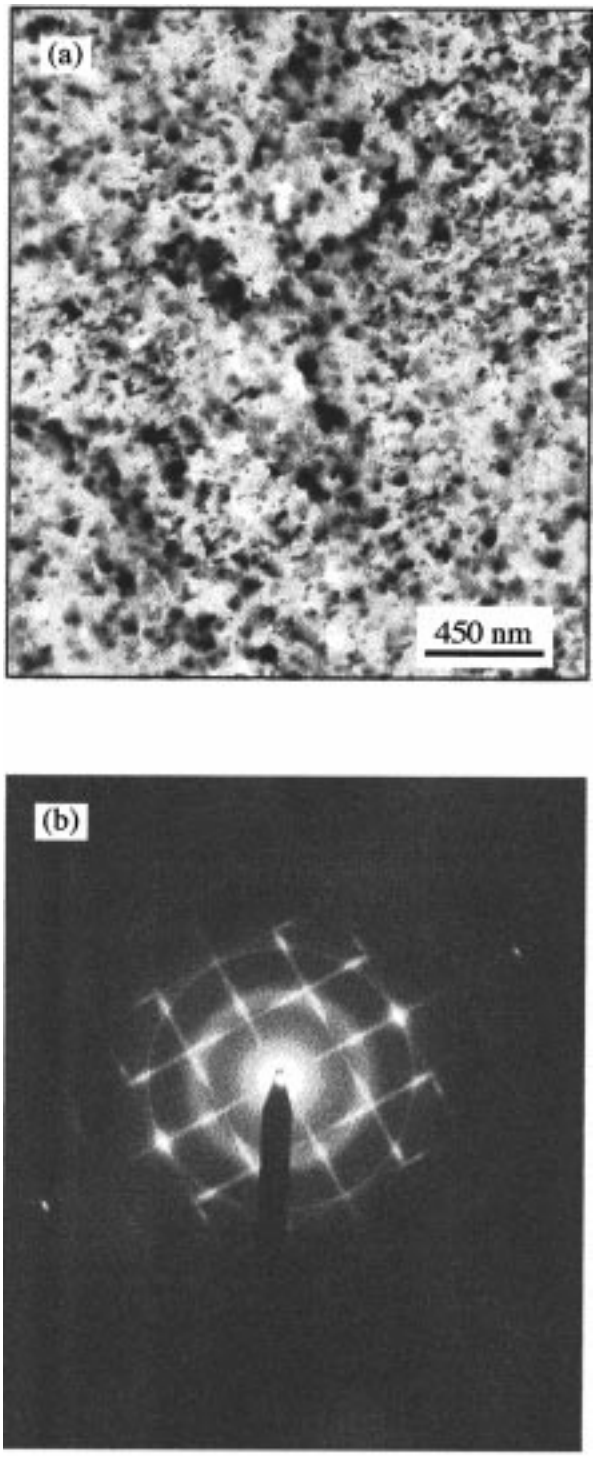

Figure 8. Bright-field TEM image (a) and associated selected area electron diffraction pattern (b) of an InSe film grown at 350 °C using $[(Me_2EtC)In(\mu_3\text{-}Se)]_4$.

potential control exerted by a precursor's molecular structure over the composition, structure, and morphology of a MOCVD thin film. In particular we are interested as to their advantages (and disadvantages) over traditional multisource systems, i.e., the use of separate precursors for each of the components of the desired thin-film material. With regard to the results described herein and given the vast literature pertaining to single-source precursor MOCVD, it is worth asking the following questions: Do single-source precursors *solely* function as a means of efficiently transporting elements to a surface? If yes, then what makes one compound more efficient than another? If no, how does their use differ from traditional multisource MOCVD or physical vapor deposition (PVD)?

With regard to the formation of indium selenide (InSe), MOCVD growth of stoichiometric phase pure InSe may be accomplished using $[(Me_2EtC)In(\mu_3\text{-}Se)]_4$ at growth temperatures of 260−350 °C; see Table 1. This is in contrast to the growth of indium selenide thin films by PVD methods, in which the volatility of selenium requires that an excess of selenium be employed (Se/In ratio of 1.2), and even then stoichiometric films are formed only at 240 °C.[16] Thus, the range of vapor-phase composition that results in the formation of the desired phase is narrow.[37] However, the use of single-source precursors with an In:Se ratio of 1:1 does not guarantee that this ratio is extended to the thin film. Thus, while $[Me_2In(\mu\text{-}SePh)]_2$,[23] $[(^tBu)_2In(\mu\text{-}Se^tBu)]_2$, $[(^tBu)In(\mu_3\text{-}Se)]_4$, and $[(Me_2EtC)In(\mu_3\text{-}Se)]_4$ all contain an In:Se ratio of 1:1, only $[(Me_2EtC)In(\mu_3\text{-}Se)]_4$ and $[Me_2In(\mu\text{-}SePh)]_2$ at high growth temperatures (>408 °C) give stoichiometric InSe thin films. The differences between $[(^tBu)_2In(\mu\text{-}Se^tBu)]_2$ (nonstoichiometric) and $[(Me_2EtC)In(\mu_3\text{-}Se)]_4$ (stoichiometric) may be related to the structure of the precursor, i.e., the number and types of bonds that must be broken to form InSe. The dramatic difference between $[(^tBu)In(\mu_3\text{-}Se)]_4$ and $[(Me_2EtC)In(\mu_3\text{-}Se)]_4$ must involve more subtle effects, e.g., compound stability controlled by ligand sterics or changes in decomposition mechanism. Therefore, while not all single-source precursors are equally successful, the concept may be used as an efficient way to transport the required stoichiometric mixture to the growth surface.

It is interesting to note that growth of InSe using $[(Me_2EtC)In(\mu_3\text{-}Se)]_4$ below 300 °C results in the formation of poorly crystalline spherical particles; textured crystalline films being deposited at 350 °C. This suggests a change in the decomposition process from vapor phase (below 300 °C) to surface (at 350 °C) decomposition. Furthermore, the morphology of the films grown at 350 °C using $[(Me_2EtC)In(\mu_3\text{-}Se)]_4$ (Figure 8a) and $[(^tBu)_2In(\mu\text{-}Se^tBu)]_2$ (Figure 3b) are distinct and therefore clearly not as a result of the crystallization of amorphous films. Therefore, the use of single-source precursors can result in widely varying film morphology.

Experimental Section

The precursors, $[(^tBu)_2In(\mu\text{-}Se^tBu)]_2$, $[(^tBu)In(\mu_3\text{-}Se)]_4$, and $[(Me_2EtC)In(\mu_3\text{-}Se)]_4$ were prepared according to previously published procedures.[27] Compounds were stored under nitrogen but manipulated in air for transfer to the CVD chamber.

The volatilites of $[(^tBu)_2In(\mu\text{-}Se^tBu)]_2$, $[(^tBu)In(\mu_3\text{-}Se)]_4$, and $[(Me_2EtC)In(\mu_3\text{-}Se)]_4$ were determined by thermogravimetic analysis (Seiko TG/DTA 900) under argon flow and dynamic vacuum (<200 mTorr) conditions. TEM was performed on a Philips EM420 analytical electron microscope operating at 120 kV. The as-deposited films were analyzed using X-ray powder diffraction (Siemens $\theta-2\theta$ and a Scintag D5000). Compositional analysis was performed using wavelength-dispersive spectroscopy (Cameca SX 50 Microprobe) relative to calibrated standards.

Chemical Vapor Deposition Studies. Film deposition was performed using the horizontal flow CVD system (Figure

(37) It should be noted that In_2Se_3 may be readily prepared by both CVD and PVD methods.

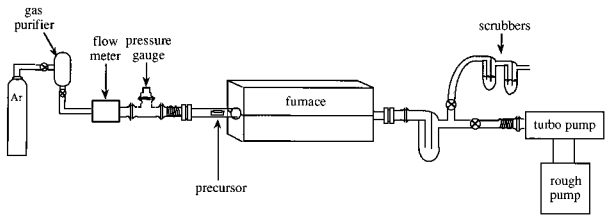

Figure 9. Schematic of experimental system for MOCVD studies using $[(^t\text{Bu})_2\text{In}(\mu\text{-Se}^t\text{Bu})]_2$ and $[(\text{R})\text{In}(\mu_3\text{-Se})]_4$.

9) previously described in detail.[6,29] The system was designed to allow deposition under dynamic vacuum conditions (10^{-3} Torr base pressure) or reduced pressure with Ar carrier gas. Argon was passed through a Cr/Cr_2O_3 gas purifier prior to entry into the chamber. The substrates were loaded into the Pyrex reactor tube and positioned in the center of the furnace and deposition temperatures and flows were adjusted such that film growth was centered on or near the substrates. Substrates consisted of freshly cleaved KBr single crystals, quartz, and Si(100) wafers. Silicon (100) and GaAs (100) substrates were cleaned with 10% HF in ethanol and rinsed with deionized water, while fused quartz substrates were rinsed with acetone prior to use. The CVD system was purged with prepurified argon (99.999%) for at least 2 h prior to deposition, during which time the hot zone was brought to the deposition temperature.

In a typical deposition experiment the CVD chamber loaded with the substrate was heated to the desired deposition temperature and purged with argon for about 1 h prior to deposition. After the system had reached thermal equilibrium, the precursor (ca. 50 mg) was then heated to the desired volatilization temperature as determined by TGA measurements. The deposition runs, typically less than 20 min, were halted within a few minutes of observing a visible coating on the KBr substrates. This resulted in films thin enough for transmission electron microscopy (ca. 300 Å). The important parameters used in the deposition are detailed in Table 1.

Acknowledgment. This work was supported by the National Science Foundation and the Office of Naval Research.

CM970638I